

Intensity Dependence of X-Ray-Induced Strain and Coloration in KCl at Room Temperature*†

EDWARD ABRAMSON‡ AND M. E. CASPARI

Department of Physics, University of Pennsylvania, Philadelphia, Pennsylvania

(Received 25 May 1962; revised manuscript received 11 October 1962)

The rate of generation of F centers and the induced external strain rate of Harshaw KCl crystals irradiated at room temperature with 46-kVp x rays have been investigated as a function of the incident radiation power density. The influence of linear plastic deformation on these two rates has also been studied. The F -center concentration was determined by standard optical techniques, and the radiation-induced strain was measured by using a capacitance-type, temperature-compensated dilatometer with a sensitivity of approximately 1 Å. It was found that the rate of slow-stage F -center generation varied as the 1.4 power of the incident intensity, in substantial agreement with the results reported by Mitchell, Wiegand, and Smoluchowski, and that the strain rate varied linearly with the intensity. A further set of experiments in which the ratio of the slow-stage F -center generation rate to the strain rate was investigated directly yielded the observation that this ratio varied as the approximately 0.7 power of the intensity. These three intensity dependences are consistent within experimental error. The discrepancy between the intensity dependences of the rates of coloration and vacancy generation is explained on the basis of a significant self-bleaching of radiation-induced color centers as reported by Schultz. The deformation experiments yielded the observation that, for the crystals used, deformation had a negligible effect on the coloration rate. From this observation and from a comparison of the observed strain rate with that predicted by the various mechanisms for defect generation by ionizing radiation which have been proposed in the literature it is suggested that the predominant mechanism, at least for the crystals used in this study, is most likely one of the bulk multiple ionization mechanisms initiated by an inner shell ionization followed by an Auger transition.

I. INTRODUCTION

THE growth curve representing the concentration of F centers generated in alkali halides at room temperature by ionizing radiation as a function of time generally exhibits two distinct regions: a saturating, relatively rapid initial rise followed by a steadier and slower increase. Depending upon the irradiation conditions, this latter region may or may not contain an inflection point.^{1,2} It is believed that the fast stage is limited by the rate at which electrons can be captured by the negative-ion vacancies present in the crystal prior to irradiation, and that the slow stage is primarily limited by the rate at which fresh negative-ion vacancies can be generated by the incident radiation.^{2,3} Furthermore, it is possible to explain the observations of the inflection point by considering the time required for a generated vacancy to capture an electron.²

That fresh vacancies can indeed be generated by ionizing radiation has been amply demonstrated by numerous investigations of the change in density⁴⁻⁶ and

linear dimensions⁶⁻¹³ associated with such irradiation. Since the photon and electron energies used in these experiments were too low, often by two orders of magnitude, to have produced vacancies by direct ion displacement, a number of mechanisms for point-defect generation, all involving the excitation of electrons, have been proposed: Seitz^{14,15} and Markham¹⁶ have discussed a process in which the energy liberated by the multiphonon recombination of an exciton may be utilized in the evaporation of vacancies from jogs in edge dislocation lines. Later, Varley¹⁷ suggested an entirely different mechanism in which the electrostatic energy of a multiply ionized halogen ion, aided by lattice vibrations, may be instrumental in causing the displacement of an ion from its normal site to an interstitial position. Although Dexter¹⁸ has raised considerable doubt as to the validity of the detailed process as originally pro-

than radiative coloring, it does demonstrate a relationship between density changes and the concentration of introduced F centers.

⁶ D. Binder and W. J. Sturm, Phys. Rev. **96**, 1519 (1954).

⁷ C. R. Berry, Phys. Rev. **98**, 934 (1955).

⁸ W. Primak, Phys. Rev. **112**, 1075 (1958); W. Primak, C. J. Delbecq, and P. J. Yuster, *ibid.* **98**, 1708 (1955).

⁹ D. Binder and W. J. Sturm, Phys. Rev. **107**, 106 (1957).

¹⁰ K. Sakaguchi and T. Suita, Technol. Rept. Osaka Univ. **2**, 177 (1952).

¹¹ L. Y. Lin, Phys. Rev. **102**, 968 (1956).

¹² H. Rabin, Phys. Rev. **116**, 1381 (1959).

¹³ D. A. Wiegand and R. Smoluchowski, Phys. Rev. **110**, 991 (1958); **116**, 1069 (1959); M. F. Merriam, D. A. Wiegand, and R. Smoluchowski, *ibid.* **125**, 52 (1962).

¹⁴ F. Seitz, Phys. Rev. **80**, 239 (1950).

¹⁵ F. Seitz, Rev. Mod. Phys. **26**, 7 (1954), particularly Secs. 10 and 37.

¹⁶ J. J. Markham, Phys. Rev. **88**, 500 (1952).

¹⁷ J. H. O. Varley, Nature **174**, 886 (1954); J. Nuclear Energy **1**, 130 (1954).

¹⁸ D. L. Dexter, Phys. Rev. **118**, 934 (1960).

* Submitted by one of the authors (E. A.) to the faculty of the University of Pennsylvania in partial fulfillment of the requirements for the degree of Doctor of Philosophy.

† This work was supported by a contract with the Electronic Technology Laboratory, Wright Air Development Division, Air Research and Development Command, U. S. Air Force. The initial support of the AFOSR. U. S. Air Force is also gratefully acknowledged.

‡ Present address: Central Research Department, Experimental Station, E. I. du Pont de Nemours and Company, Wilmington, Delaware.

¹ H. W. Etzel and J. G. Allard, Phys. Rev. Letters **2**, 452 (1959).

² P. V. Mitchell, D. A. Wiegand, and R. Smoluchowski, Phys. Rev. **121**, 484 (1961).

³ R. B. Gordon and A. S. Nowick, Phys. Rev. **101**, 977 (1956).

⁴ I. Estermann, W. J. Leivo, and O. Stern, Phys. Rev. **75**, 627 (1949).

⁵ H. Witt, Nachr. Akad. Wiss. Göttingen, Math.-Physik Kl. **IIA**, 17 (1952). While this experiment involved electrolytic rather

posed by Varley, subsequent suggestions¹⁹⁻²¹ have provided alternate, and more probable, steps by means of which multiple ionization might lead to ion displacement. The multiple ionization itself appears to be the result of an inner shell ionization followed by an Auger transition.^{21,22}

Recently, Mitchell *et al.*² observed that the rate of increase of the peak absorption coefficient of the *F* band in KCl during the slow stage of coloration at room temperature, described by the parameter a^* , varied as the square of the intensity of irradiation. From their analysis, this parameter a^* is proportional to the rate at which fresh vacancies are being generated and filled with electrons corrected for the rate at which the *F* centers so formed are being bleached. By arguing that the bleaching correction is negligibly small, the authors concluded that the rate of generation of fresh vacancies was proportional to a^* , and hence to the intensity squared. In order to explain this and other observations, they suggested a damage mechanism in which two exciton recombinations, both taking place at the same halogen ion located at the core of an edge-dislocation line and both occurring within a characteristic time interval, might result in the evaporation of a vacancy from the dislocation line.

In Fig. 1 we have plotted a^*/I as a function of I , where I is the intensity of irradiation from the data of Mitchell *et al.* This form is more sensitive than the log-log plot exhibited by these authors to the existence of a nonlinear relationship. If a^* is proportional to the square of the intensity, then the points of this graph should lie close to a straight line passing through the origin. Although the points are not incompatible with such a straight line, it was felt that the data was not entirely conclusive. Accordingly, it was decided that the rate of generation of fresh vacancies in potassium chloride at room temperature would be re-investigated with the highest possible accuracy.

In addition to repeating the intensity-dependence studies of Mitchell *et al.*, we have measured the radiation-induced linear expansion of KCl at room temperature as a function of intensity. Since the presence or absence of an electron in a negative ion vacancy has been shown to have a negligible effect on the dilation of the lattice,¹¹ the expansion technique has the advantage of being unaffected by factors such as the initial fast coloration, the bleaching of *F* centers, or the formation of *F* centers from vacancies. The interpretation of the data in terms of the rate of vacancy production does, however, require the assumption that the induced external strain is linearly related to the concentration of generated vacancies.

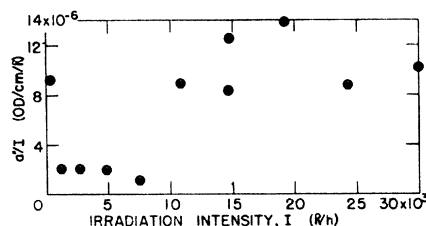


FIG. 1. a^*/I vs intensity of irradiation in KCl at room temperature. The quantity a^*/I is proportional to the efficiency of slow-stage *F*-center generation. The unit OD is defined as $\log_{10} T_m$, where T_m is the percent optical transmission of the crystal at the peak of the *F* band. (Mitchell, Wiegand, and Smoluchowski, reference 2.)

The proposed mechanisms for the generation of vacancies by ionizing radiation cited above involve either the production of interstitials or the climb of the extra half-planes of dislocations. In either case, a plausible argument can be made that these processes result in the external dilation of the crystal. Although order-of-magnitude estimates can be made, the precise relationship between this dilation and the concentration of generated vacancies is not known, and may, in fact depend upon the type, purity, and perfection of the crystal, as well as on the type of defect produced and the temperature at which the irradiation is performed. Whether or not the relationship is exactly linear in the concentration of generated vacancies is itself open to question on conceptual grounds. Consider, for instance, the coagulation of two negative ion vacancies into the *M* center structure.²³⁻²⁵ Although isolated vacancies as such do not seem to contribute significantly to the external dilation,¹³ it is possible that a relaxation of the lattice will occur around such coagulations of vacancies. Such a relaxation would, in the case of *M* centers, introduce a second-order term into the relationship between external strain and the concentration of generated vacancies. A similar argument can be applied to higher-order coagulation centers. As long as the concentrations of these coagulation centers are small compared to the concentration of *F* centers, however, the second- and higher-order terms can be neglected. It has been shown experimentally²⁴ that this condition is fulfilled for *F* center concentrations lower than $10^{18}/\text{cm}^3$.

II. EXPERIMENTAL DETAILS

A. Samples

All of the individual samples used in this experiment were cleaved from a single boule of KCl obtained from the Harshaw Chemical Company. Their size was approximately $13 \times 8 \times 1$ mm, they were irradiated parallel to their shortest dimension, and their dilation was measured along their longest dimension.

¹⁹ C. C. Klick, Phys. Rev. **120**, 760 (1960).
²⁰ R. E. Howard, S. Vosko, and R. Smoluchowski, Phys. Rev. **122**, 1406 (1961).
²¹ F. E. Williams, Phys. Rev. **126**, 70 (1962).
²² J. Sharma and R. Smoluchowski, Bull. Am. Phys. Soc. **7**, 178 (1962).

²³ C. Z. van Doorn, Philips Res. Rept. **12**, 309 (1957).
²⁴ B. J. Faraday, H. Rabin, and W. D. Compton, Phys. Rev. Letters **7**, 57 (1961).
²⁵ E. Sonder, Phys. Rev. **125**, 1203 (1962).

Most of the crystals employed for the intensity-dependence studies were used in the "as-received" condition, that is, without any treatment beyond the cleaving operation. Two samples, however, had different histories: One, after its as-received, intensity-dependence measurements had been taken, was subjected to a 4-h anneal at 450°C followed by slow cooling at a rate not exceeding 6°C/h. The intensity dependence of the radiation-induced strain of this crystal was then re-measured. The other sample had its ends ground, as shown in the inset to Fig. 10, thus insuring that the measured expansion was more typical of the bulk crystal than of the front surface.

The crystals used in the plastic deformation studies were linearly compressed along their longest dimension in a hand vise. Although those which appeared obviously bent, nonuniformly strained, or cracked were discarded, it is possible that the crystals finally used contained some nonuniformity. Strict control of the compression process was not employed, however, since the nature of the results (see below) did not warrant such care.

B. Dilatometer and Detection Equipment

The sample capacitor used in the dilatometer is shown in isometric projection in Fig. 2. This type of construction, in which the bottom of the upper plate and the top of the lower plate are supported by nearly identical lengths of identical materials, results in a high degree of thermal compensation, or insensitivity to small tem-

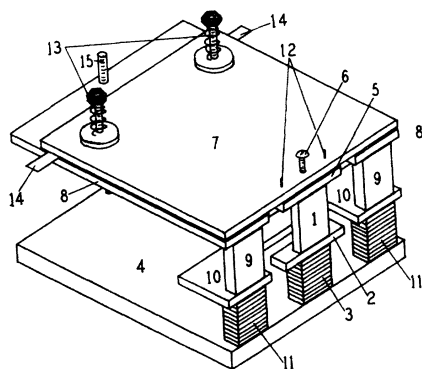


FIG. 2. Dilatometer capacitor. The crystal under observation (1) sits on a brass plate (2), which in turn rests upon a stack of quartz plates (3) and a base plate (4). The quartz plates are used for the calibration procedure mentioned in the text. The top of the sample supports a tool steel plate (5), upon which rests a fine steel screw threaded through the upper capacitor plate (7) made from precision ground flat tool steel. The screw is used for fine adjustment of the capacitor air gap. The other capacitor plate (8), also made from precision ground flat tool steel, is supported by two crystals (9) identical in composition and length to crystal (1). These crystals rest, in turn, upon a brass plate (10) identical in thickness to plate (2), two stacks of quartz plates (11) each identical to stack (3), and the base plate (4). The steel pins (12) serve as guide rods for plate (5). At their back end, the two capacitor plates are held together by spring loaded screws passing through insulating bushings (13). A piece of 0.002-in.-thick mica (14) serves as an insulating spacer between the back ends of the two plates. The rear of the capacitor assembly is supported above the base plate by a long screw (15).

perature fluctuations. The major contribution to the slight unavoidable miscompensation comes from the mica and steel spacers required to maintain the air gap.

The capacitor served as the unknown in a commercial capacitance bridge and detector operating at 455 kc modulated at 1.2 kc, the output of which was fed into a strip chart recorder. During an experiment, the two support pieces of KCl (9 in Fig. 2) were shielded by $\frac{3}{8}$ -in. lead, and hence only the sample crystal received radiation. Any irradiation-induced change in length of this crystal resulted in a corresponding change in the separation between the capacitor plates, and the accompanying capacitance change appeared as a deviation of the recorder pen. Since the bridge output was linear for the small changes in capacitance encountered, the pen deviation was linearly related to the length changes. This latter linearity was checked by employing the calibration procedure to be described below at both ends of the recorder scale.

The plates of the dilatometer capacitor were approximately 3 in. square, and their separation could easily be adjusted to be 0.01 cm; hence the nominal capacitance between them was 500 $\mu\mu\text{F}$. The detection equipment, including the recorder, was capable of displaying capacitance changes as small as approximately 0.0001 $\mu\mu\text{F}$. As can be readily verified, the relationship between the change in plate separation d and the change in capacitance C of a parallel plate capacitor is $\Delta d = -d\Delta C/C$; hence, the ideal sensitivity of the entire system to changes in plate separation was approximately 0.2 Å. Although the sample was mounted on a vibration damping support, the noise arising from building vibrations, which had a period of less than a second, could not be reduced below an amplitude of 1 Å. Since, however, the time of a single observation was an hour or two, this noise did not markedly affect the sensitivity.

The response of the recorder pen was correlated with the change in plate separation by using the piezoelectric expansion of the quartz plates labeled (3) in Fig. 2. These plates were arranged so that an applied potential difference of a few hundred volts would result in a change of plate separation of the order of 100 Å.

C. Temperature Controls

The error in the thermal compensation of the sample capacitor caused by the material required to maintain an air gap of 0.01 cm between the capacitor plates was equivalent to a residual thermal expansion of 10 Å/°C. Therefore, in order that the sensitivity of the measuring apparatus could be realized, it was necessary to reduce the temperature fluctuations in the vicinity of the capacitor to 0.01°C. This was effected by placing the capacitor in an oven whose walls were made of 1-in.-thick styrofoam, and in which the temperature was regulated by a proportional controller using a nickel resistance thermometer as its sensor.

The capacitors used in the bridge had temperature

coefficients of zero plus or minus 30 parts per million per °C. Since it was desired to detect changes in the capacitance of the sample capacitor as small as 2 parts per million, the bridge was thermostated to approximately 0.05°C. In addition, in order to improve the gain stability of the amplifier, it was thermostated to approximately 0.5°C. The thermal stability of the entire detecting system was checked by substituting a dummy capacitor for the crystal capacitor, and was found to be completely stable for a 3-h test period at the highest sensitivity.

D. Irradiation

1. Source and Geometry

The radiation used in this experiment was generated in a Matchlett x-ray tube having a molybdenum target. The tube was operated at 46 kVp and at currents ranging up to 20 mA by a Picker diffraction generator with a half-wave rectifier circuit. The port of the tube was placed 2 in. from the sample, and the beam was filtered by 1 in. of styrofoam (the oven insulation) and 0.012 in. of aluminum. While the aluminum filter used was about $\frac{1}{10}$ the thickness of those commonly employed to remove the softer components of the radiation and thus insure relatively uniform body coloration, the use of a thicker filter would have reduced the incident power density of the beam to a value inconveniently low for some parts of the experiment. For the sake of constancy of the quality of the radiation, it was decided that the thin filter would be used at all times. One part of the experiment was specifically designed to test for the effects of nonuniform body coloration. This matter is discussed in detail below.

2. Stabilization

Since the crux of the experiment was to measure the rate of expansion of a crystal as a function of the intensity of irradiation, it was necessary to reduce the

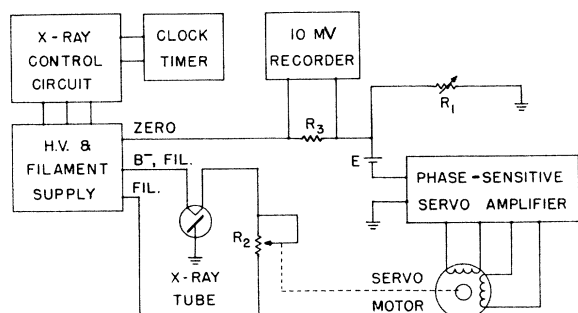


FIG. 3. Servo system for x-ray tube current stabilization. The tube plate current passed through reference resistor R_1 . The potential difference so developed was compared to a standard emf, E , which, in turn, drove the servo motor. This servo motor was linked to the filament control of the x-ray circuit, R_2 , and adjusted the filament temperature so as to keep the tube current constant. The clock timer controlled the exposure intervals, and the recorder was used to monitor the tube current.

variations in the x-ray tube plate current, to which the beam intensity is proportional, to a minimum. This was done by employing the servo-control system shown in the block diagram of Fig. 3. The reference resistor R_1 was variable, its value determining the tube current. This system was able to limit the peak-to-peak fluctuations of the plate current to within 3% of its average value. The 10-mV recorder was used to continuously monitor the tube current, and served as the primary indicator of the radiation intensity.

3. Measurement and Calibration of Incident Power Density.

As long as the plate voltage of the x-ray tube is held fixed, the radiation intensity can be considered to be directly proportional to the plate current. In order that physical calculations can be performed, this plate current must be converted into some standard unit of intensity, which, for this investigation, was chosen to be the power density of the beam in either W/cm^2 or $erg\ cm^{-2}/sec$. The conversion factor was determined through the following procedure:

Three pieces of lead, each measuring $10 \times 10 \times 1$ mm, were inserted into the dilatometer capacitor in place of the KCl samples. This thickness of lead will absorb 99.9988% of incident primary photon radiation at 46 keV. The center slab of lead (position 1 in Fig. 2) had attached to it four wires, arranged for electrical power dissipation measurements. X rays were allowed to fall upon this central slab, and its resulting thermal expansion was measured by noting the steady-state change in capacitance between the plates. The x rays were then turned off and the thermal expansion duplicated by internal joule heating. Care was taken that the surroundings of the lead slabs, and hence the heat loss mechanisms, remained unchanged throughout the series of measurements. The results so obtained are displayed in Fig. 4 in which the calculated incident power density S is plotted against the x-ray tube plate current,

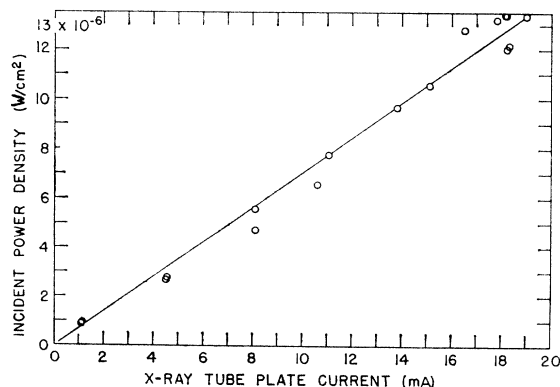


FIG. 4. Calibration of the incident x-ray power density for the irradiation used in the strain measurements. The line has been fitted by the least-squares method, and has a slope equal to $(0.70 \pm 0.02) \times 10^{-6} W/cm^2/mA$.

I. The slope of the least-squares fitted line is $S/I = (0.70 \pm 0.02) \times 10^{-6} \text{ W} \cdot \text{cm}^{-2}/\text{mA}$.

E. X-Ray Absorption Coefficient of Samples

The procedure described above for measuring the incident power density of the beam was easily adapted to the determination of the effective x-ray absorption coefficient of a sample: The thermal expansion of the central lead slab was observed both with and without the sample under investigation in the beam. The effective absorption coefficient was then calculated from

$$\langle \mu \rangle = -(1/t) \ln(X/X_0), \quad (2.1)$$

where t was the thickness of the sample, X_0 the thermal expansion of the lead slab with no sample in the beam, and X the expansion with the sample in the beam. The results of these measurements are displayed in Fig. 5(a). The x rays used in this experiment were not monochromatic, hence, as a result of the stronger absorption of the lower energy components, the measured absorption coefficient decreases with increasing sample thickness.

For energies removed from characteristic absorption edges, the x-ray absorption coefficient of a material varies according to the relationship²⁶

$$\mu = a + b/(h\nu)^3, \quad (2.2)$$

where a and b are constants which can be derived from tables of the absorption coefficient as a function of x-ray

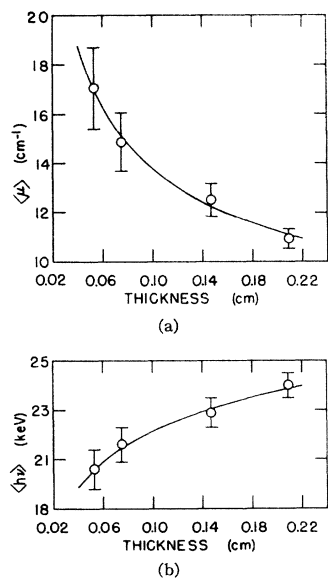


FIG. 5. (a) Effective x-ray absorption coefficient of KCl, $\langle \mu \rangle$, and (b) effective photon energy, $\langle h\nu \rangle$, vs KCl crystal thickness (determined for the irradiation used in the strain measurements). The curves represent least-squares fits of the equations $\langle \mu \rangle = A + Bt^{-1/2}$ and $\langle h\nu \rangle = (C + Dt^{-1/2})^{-1/3}$ [L. Silberstein, *Phil. Mag.* **15**, 375 (1933).]

²⁶ G. L. Clark, *Applied X-Rays* (McGraw-Hill Book Company, Inc., New York, 1955), 4th ed., p. 165.

energy. From the values of these constants for KCl, and from the measured values of $\langle \mu \rangle$, an effective photon energy of the beam, $\langle h\nu \rangle$, was calculated, as displayed in Fig. 5(b). Both $\langle \mu \rangle$ and $\langle h\nu \rangle$ will be used later in an attempt to estimate the order of magnitude of the strain rate which one might expect on the basis of the various mechanisms of defect generation.

F. Optical Absorption Measurements

All optical absorption measurements were taken at room temperature on a Perkin Elmer model 4000A Spectracord operated in a wavelength range extending from 1150 to 420 μ . This included the R , M , and N bands as well as the F band. The measurements were not corrected for reflection since the accuracy of the rest of the experiment did not warrant such care. From the F band so observed, the concentration of F centers was calculated by using Smakula's equation²⁷ with an oscillator strength of 0.81. The samples were handled either in total darkness or under weak red light to preclude possible optical bleaching. The bleaching caused by the measuring light was observed to be negligible.

G. Experimental Procedure

Before being exposed to radiation, each fresh sample was examined optically in the Spectracord, after which it was inserted into the sample capacitor. Following a wait during which the sample oven came to equilibrium, the irradiation was commenced. This irradiation consisted of periods of exposure alternated with equal periods of no exposure, the total time for one cycle usually being 3 h. During those parts of the experiment in which the intensity dependence of the strain rate was being tested, the x-ray tube current was varied between a small number of preselected values from exposure to exposure. Each sample was irradiated a large number of times without being removed from the dilatometer, with care being taken that the total dose did not become so great that saturation effects could be noticed. When strain measurements (for a given nominal intensity)

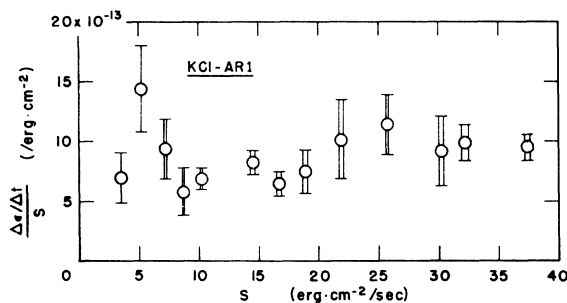


FIG. 6. The macroscopic, radiation-induced specific strain rate, $(\Delta \epsilon / \Delta t) / S$, of as-received Harshaw KCl x irradiated at room temperature vs the incident power density, S .

²⁷ A. Smakula, *Z. Physik* **59**, 603 (1930), cited in F. Seitz, *The Modern Theory of Solids* (McGraw-Hill Book Company, Inc., New York, 1940), Eq. (8), p. 664.

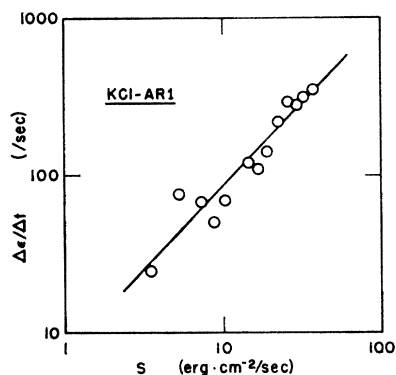


FIG. 7. The macroscopic, radiation-induced strain rate, $\Delta\epsilon/\Delta t$, of as-received Harshaw KCl x irradiated at room temperature vs the incident power density, S .

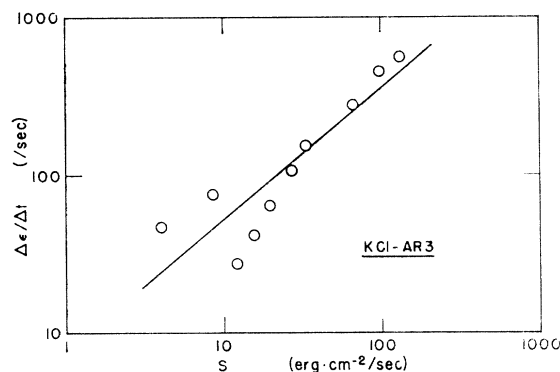


FIG. 8. The macroscopic, radiation-induced strain rate, $\Delta\epsilon/\Delta t$, of as-received Harshaw KCl x irradiated at room temperature vs the incident power density, S .

taken at the beginning and end of an entire series of exposures were compared, saturation could not be detected. The crystals were kept in the dark throughout the complete set of exposure cycles, and were irradiated so that the final concentration of F centers was less than $10^{17}/\text{cm}^3$. During the irradiations, the entire measuring system was periodically calibrated according to the procedure described above.

During the irradiation cycles, the output of the capacitance bridge was continuously monitored on the strip-chart recorder. The slope of this recorder trace was proportional to the rate of change of the capacitor plate separation, and hence of the sample length. This slope was not zero during the "exposure off" portions of the cycles, but indicated a slight, continuous contraction which was attributed to slow plastic deformation. The radiation-induced expansion rate of the crystal was taken as the difference between the slopes of the "exposure on" and "exposure off" portions of the trace. The x-ray tube plate current was also continuously monitored.

The samples were given from 3 to 25 exposures at each selected nominal intensity. For each exposure, the strain rate $\Delta\epsilon/\Delta t$ and the specific strain rate $(\Delta\epsilon/\Delta t)/S$ were calculated. Then, for each nominal intensity the mean incident power density S and the mean specific strain rate were calculated and graphed. The standard deviations of these means were also calculated and used as the quoted errors of the measurements. Independent

estimates of the errors, based on the accuracy with which the recorder traces could be interpreted, were in agreement with the calculated standard deviations.

III. RESULTS

A. Macroscopic Strain Rate vs Intensity

The specific macroscopic strain rate $(\Delta\epsilon/\Delta t)/S$ of a representative as-received KCl crystal (sample AR1) irradiated at room temperature is plotted against the incident power density of the x-ray beam in Fig. 6. As can be seen, there is no tendency for the points to go through the origin, which would be the expected behavior if the strain rate $\Delta\epsilon/\Delta t$ were proportional to the intensity to a power greater than one. The results for another as-received crystal showed the same form. The power of S to which the macroscopic strain rate is proportional can be most easily ascertained from a log-log plot of the data. Accordingly, the strain rates of both samples have been plotted in this form in Figs. 7 and 8. The least-squares method has been used to fit straight lines to the points in these graphs. The slopes of these lines, along with a similar slope from data to be presented shortly, are tabulated in Table I, in which the quoted error in the slope has been calculated from the error associated with each point. Note that these slopes are, within the error limits, equal to unity.

If it is assumed that the strain rate is linearly proportional to the incident power density, then an aver-

TABLE I. Data from intensity-dependence measurements.^a

Sample	b	\bar{y} (/erg cm ⁻²)	Treatment	Total incident dose (erg cm ⁻²)	Final concentration of F centers (cm ⁻³)
KCl-AR1	1.1 ± 0.1	$(8.9 \pm 0.7) \times 10^{-13}$	as-received	1.0×10^7	3.3×10^{16}
KCl-AR3	0.8 ± 0.3	$(5.1 \pm 1.0) \times 10^{-13}$	as-received	0.9×10^7	5.0×10^{16}
KCl-AR3AN	0.8 ± 0.3	$(3.4 \pm 0.3) \times 10^{-13}$	irradiated, annealed	0.5×10^7 ^b	1.8×10^{16} ^b

^a b = Power of S in relationship $(\Delta\epsilon/\Delta t) \propto S^b$; \bar{y} = average value of $(\Delta\epsilon/\Delta t)/S$ under the assumption that $b = 1$.

^b After the anneal.

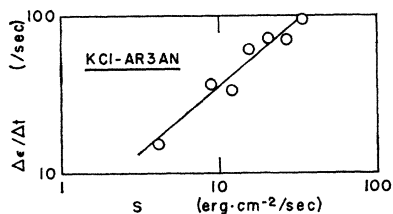


FIG. 9. The macroscopic, radiation-induced strain rate, $\Delta\epsilon/\Delta t$, of irradiated then annealed Harshaw KCl at room temperature vs the incident power density, S .

age value of the specific strain rate, which has been assumed to be proportional to the efficiency of defect generation, can be calculated from data of the form presented in Fig. 6. These averages for both crystals have been included in Table I. The error quoted is the standard deviation of the mean.

Sample AR3 was annealed as previously described and then re-irradiated, the specific strain rate so obtained being similar in form to Fig. 6. The data for this crystal is presented in Fig. 9, and included in Table I.

It is a characteristic of the dilatometric system used in this investigation that if the expansion of the crystal under examination is nonuniform throughout its thickness, only the largest expansion is measured. Since the x rays used for the irradiation were not very highly filtered and consequently contained much of the softer components, a large part of the incident energy was absorbed near the front surface of the sample. Hence this front surface experienced a larger expansion than the bulk of the crystal. In order to ascertain whether or not this preferential front surface absorption had any effect on the nature of the results, the following experiment was performed:

The two ends of a crystal which would come in contact with the dilatometer capacitor were ground as shown in the inset to Fig. 10. This grinding was such that only the rear quarter of the crystal ends made contact. Thus, since the sample was 0.83 mm thick, the x rays which were effective in causing the measured radiation-

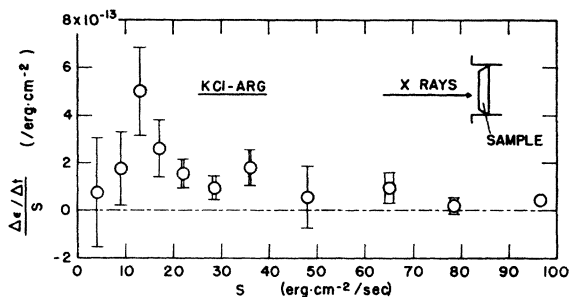


FIG. 10. The macroscopic, radiation-induced specific strain rate at room temperature, $(\Delta\epsilon/\Delta t)/S$, of Harshaw KCl ground as shown in the inset, vs the power density incident upon the front surface, S . This crystal received a total incident x-ray dose of 1.6×10^7 erg cm^{-2} and its final average F -center concentration was 9×10^{19} cm^{-3} .

induced expansion were filtered through approximately 0.6 mm of KCl. The specific strain rate of this sample is displayed in Fig. 10. Note that, just as for the samples previously mentioned, there is no indication that the points tend towards the origin. Hence, it is believed that no error was introduced by measuring the expansion near the front surface. The ground crystal method was not used throughout the experiment because of its inherently lower precision.

B. Rate of Formation of F Centers vs Intensity

An examination of the equation used by Mitchell *et al.*² to describe their F -center growth curves reveals that their parameter a^* is given by the slope of the growth curve after the crystal has received an x-ray dose approximately ten times the dose required to reach the knee of the curve. Hence, a direct check of the square-law results was performed by determining this slope for a number of crystals of matched thickness, each of which had been irradiated at a different intensity.

Since this part of the investigation was performed concurrently with the dilatometric measurements, a different radiation source was used, and hence no direct comparison of these results with those reported above can be made. The x rays used for the irradiation were generated in a copper-target tube operated at 45 kVp and 20 mA by a Norelco full-wave rectified diffraction unit, and were passed through a filter of 0.012-in. aluminum. The intensity was varied by changing the distance between the sample and the target of the tube. The procedure for the measurement of the beam power density described above could not be applied in this case; however, by appealing to the similarity between the operating conditions for this source and the source employed for the dilatometric measurements, it is estimated that the minimum incident power density used for this particular part of the investigations was approximately 1 erg $\text{cm}^{-2}/\text{sec}$. The irradiations were carried out at room temperature and in the dark, and each crystal received a total dose of approximately 10^6 erg cm^{-2} .

Periodically, the irradiation was interrupted and an optical absorption measurement was taken, also at room temperature, each measurement being completed within 5 min after the cessation of the irradiation. In this way, F -center growth curves similar to that shown in Fig. 11(a) were developed for five different intensities. It was observed that the knee of all five of these growth curves occurred at a total incident dosage of approximately 10^5 erg cm^{-2} . The slopes of these curves at total incident dosages greater than 10^6 erg cm^{-2} were then measured. This portion of the growth curve is indicated by the heavy line in the figure. These slopes $\Delta n_F/\Delta t$, having been measured at a dosage at which all of the crystal was far out in the slow stage of coloration, should correspond to the a^* of Mitchell *et al.*

That substantially all of the crystal had advanced

into the slow stage of coloration, but not into saturation, at the indicated total dosage may not be immediately obvious since the x-ray intensity must decrease as the sample is penetrated. Certainly, Fig. 11(a) suggests that most of the crystal was in the slow stage. Let us, however, make the extreme assumption that at t_k , the dose corresponding to the knee of the curve in the figure, only the irradiated surface was in the slow stage. From Fig. 5(a) it can be ascertained that the x-ray intensity at the back surface of a 0.1-cm-thick sample was 25% of the incident intensity. Hence, under the extreme assumption, the back surface should go into slow-stage coloration at a dosage not greater than $4t_k$. The measurements were taken at approximately $10t_k$. The possibility that any part of the crystal had gone into the saturation region of coloration can be ruled out by noting that the dilatometric measurements, which relate to the most heavily damaged layer of the sample, showed no evidence of saturation at the dosage in question.

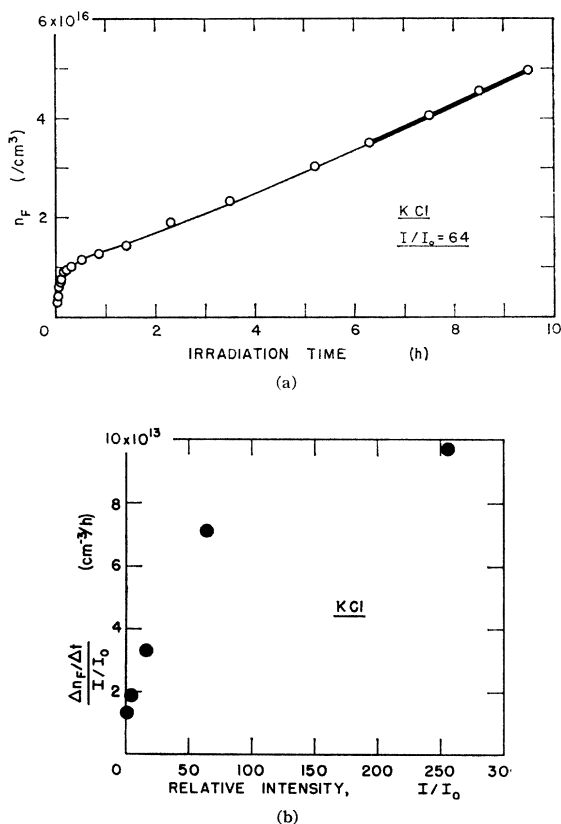


FIG. 11.(a) A representative F -center growth curve in as-received Harshaw KCl irradiated in the dark at room temperature and at a constant x-ray intensity of approximately $64 \text{ erg cm}^{-2}/\text{sec}$. The portion of the curve from which the slow-stage coloration rate, $\Delta n_F/\Delta t$, was determined is approximately indicated by the heavy line. (b) The relative efficiency of slow-stage F -center generation, $(\Delta n_F/\Delta t)/(I/I_0)$, in as-received Harshaw KCl x irradiated at room temperature vs the relative intensity of irradiation, I/I_0 , where $I_0 \approx 1 \text{ erg cm}^{-2}/\text{sec}$.

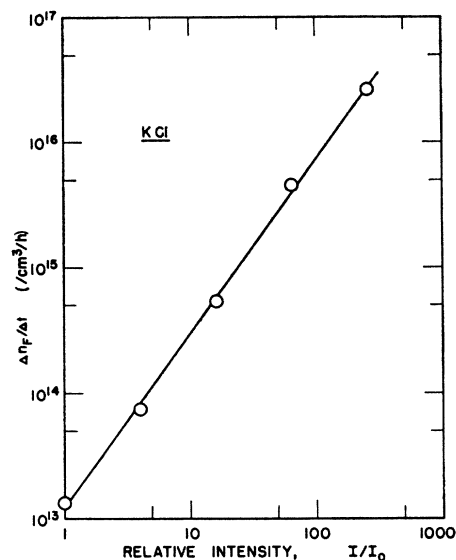


FIG. 12. The rate of slow-stage F -center generation, $\Delta n_F/\Delta t$, in as-received Harshaw KCl x irradiated at room temperature vs the relative intensity of irradiation, I/I_0 , where $I_0 \approx 1 \text{ erg cm}^{-2}/\text{sec}$.

The relative efficiencies obtained from the coloration measurements are plotted as a function of the relative incident intensity in Fig. 11(b), in which the measurement error of each point is approximately represented by the size of the point. This figure shows a definite tendency for the points to pass through the origin and hence indicates that the slow-stage rate of F -center generation is proportional to the intensity of irradiation to a power greater than one. A log-log plot of the data, shown in Fig. 12, indicates that this power is approximately 1.4, in substantial agreement with the results reported by Mitchell *et al.*

Note added in proof. P. G. Harrison [J. Chem. Phys. 37, 388 (1962)] has recently determined that the rate of slow-stage coloration of NaCl at room temperature also increases with increasing x-ray intensity.

C. Ratio of F -Center Formation Rate to Strain Rate

The data presented in the preceding two sections, that is, that the rate of generation of F -centers varies as the 1.4 power of the intensity while the strain rate is linear in the intensity, strongly suggested that these two rates be directly compared in the same crystal. Accordingly, five samples, selected to be of approximately the same thickness and from the same section of the boule, were subjected to the following set of operations: The strain rate of a sample at a particular nominal intensity was measured as previously described. The F -center concentration was then determined from optical measurements. Following this, the crystal was re-irradiated at the same nominal x-ray intensity, and its F -center concentration again determined. During all of these operations the crystal was kept at room tem-

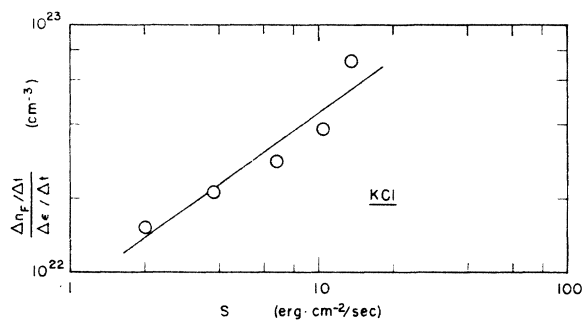


FIG. 13. The ratio between the slow-stage rate of F -center generation and the macroscopic, radiation-induced strain rate, $(\Delta n_F/\Delta t)/(\Delta \epsilon/\Delta t)$, of as-received Harshaw KCl x irradiated at room temperature vs the incident power density, S . The straight line has been fitted by the least-squares method and has a slope of 0.7 ± 0.15 .

perature and either in the dark or in weak red light. The rate of generation of F centers was determined from the last two measurements, the use of only two points in calculating this rate being justified by the precision of optical measurements and the linearity of the F -center growth curve in the slow stage. Since the crystals had received (during the strain measurements) an x -ray dose in excess of 10^6 erg cm^{-2} before the optical measurements were taken, the F center generation rate determined should have the same significance as the parameter a^* . The data so obtained is displayed in Fig. 13. The slope of this log-log plot is 0.7 ± 0.15 , where the error is one standard deviation of the slope. This value is in substantial agreement with the expected value of 0.4.

D. Influence of Plastic Deformation

Figure 14 shows the macroscopic specific strain rates of a number of crystals which had been linearly deformed by various amounts. The vertical errors shown are the standard deviations of the means, while the horizontal errors represent the estimated error in the determination of the percent deformation. It can be seen that there is no regular dependence of the strain rate on the deformation. A possible explanation for the apparent radiation-induced contraction in the neighborhood of 8% deformation is offered in Sec. IV.

In testing the influence of plastic deformation on the slow-stage coloration process, full F -center growth curves were not developed. Instead, after the strain-rate measurements on each crystal had been completed, the slow-stage F -center generation rate in that crystal was determined as described in the preceding section. An examination of the data presented by Mitchell *et al.*² reveals that the parameters describing the dosage corresponding to the knee of the growth curve (b^* and c^* in their paper) do not increase by more than a factor of 3 when the crystal is deformed. Therefore, since our crystals had received an x -ray dose of approximately 5×10^6 erg cm^{-2} prior to the performance of the coloration measurements, the F -center generation rate in

them was obtained far out in the slow stage of coloration and should correspond to the true slow-stage rate of F -center generation a^* introduced by Mitchell *et al.* The results so obtained are presented in Fig. 15, in which the horizontal errors are as described above. The errors involved in the determination of $(\Delta n_F/\Delta t)/S$ fall into three classes: The first class contains those errors arising from a misapplication of Smakula's equation²⁷ or an incorrect choice of the constants appearing therein. Being systematic errors, these can only shift all the points proportionately and hence are not depicted on the graph. The second class consists of random measuring errors which can contribute to the scatter of the data about a trend line. Since optical absorption, sample thickness, time of irradiation, and incident intensity can all be measured to better than 1% accuracy, it is estimated that the random vertical errors of this type in Fig. 15 are approximately represented by the size of the points. The fact that x rays do not produce slow-stage F centers uniformly throughout the bulk of the crystal, but rather preferentially color the front portion gives rise to the third class of error. For example, if two samples identical except for thickness were both given the same x -ray treatment, it would be expected that the thicker sample would exhibit the lower average F -center concentration as measured by standard optical techniques. If the data presented in Table II are analyzed, a crude correlation between slow-stage coloration rate and crystal thickness can be found. This correlation is evident, however, only if those samples deformed less than 7% and those deformed more than 7% are considered in two separate groups. As suggested by Fig. 14, and as further discussed in Sec. IV C, there is reason to believe that these two groups of samples should be considered separately. While it is doubtful that these thickness variations can explain all of the scatter in Fig. 15, it is probable that they can account for a considerable part of it.

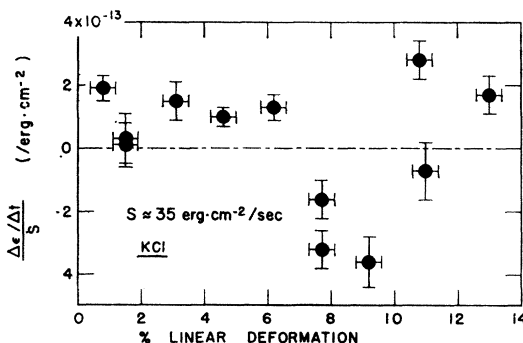


FIG. 14. The macroscopic, radiation-induced specific strain rate, $(\Delta \epsilon/\Delta t)/S$, of deformed Harshaw KCl x irradiated at room temperature vs the percent linear plastic deformation of the sample. Each crystal received a total incident dose of approximately 0.5×10^7 erg cm^{-2} during the measurements.

²⁸ C. L. Bauer, thesis, Yale University, 1959 (unpublished), cited in C. L. Bauer and R. B. Gordon, *Phys. Rev.* **126**, 73 (1962).

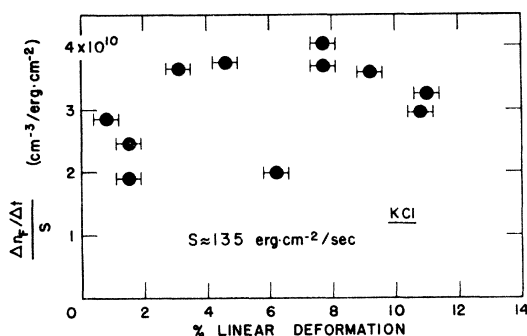


FIG. 15. The efficiency of slow-stage F -center generation, $(\Delta n_F/\Delta t)/S$, of deformed Harshaw KCl irradiated at room temperature vs the percent linear plastic deformation of the sample. Prior to the performance of these measurements, each of the crystals shown in the figure had received an incident x-ray dose of approximately 5×10^6 erg cm^{-2} . Hence the points correspond to measurements taken far out in the F -center growth curve.

It has been reported²⁸ that a 3% deformation raises the dislocation concentration (and presumably the number of incipient vacancies along dislocation lines) by a factor of about 100. As evidenced by Fig. 15, in our experiments the same deformation had little effect on the slow-stage coloration rate. That this lack of strong deformation dependence cannot be attributed to saturation of the damage process is evidenced by two observations: (1) Strain measurements on "as-received" and on lightly deformed samples show no significant saturation for the total dosages at which these measurements were made. (2) The data of the figure reveal that F centers are being generated at a respectable rate (approximately 10^{16} cm^{-3}/h). Hence, it is suggested that of the vacancy-generation mechanisms proposed in the literature,¹⁴⁻²¹ those requiring the presence of dislocations did not contribute significantly to the slow-stage coloration rate observed in the crystals investigated here.

IV. DISCUSSION

A. Comparison of Strain Rate and Coloration Rate

The results reported above strongly indicate that the production of vacancies and the slow-stage generation of F centers by radiation do not have the same functional dependence on the intensity of the radiation. In particular, it appears that while the rate of generation of vacancies is linear in the incident intensity (under the assumption that the induced strain is directly proportional to the concentration of generated vacancies), the slow-stage coloration rate varies as approximately the 1.5 power of the intensity. The dissimilarity in the functional dependence of these two phenomena can be explained by examining the parameter a^* , introduced by Mitchell *et al.*,² which is proportional to the observed slow-stage coloration rate. This parameter is actually a combination of three other parameters, that is,

$$a^* = ac/(\beta + c), \quad (4.1)$$

where a describes the rate of vacancy generation, c is the rate at which a vacancy captures an electron and hence becomes an F center, and β is a rate constant describing the bleaching of F centers. Mitchell *et al.*, by arguing that β is negligible compared to c , set $a^* \approx a$, and hence conclude that a^* is proportional to the rate of generation of vacancies.

The parameter c can be rewritten as $c = B_V n_e$, where B_V is the capture coefficient for electrons by negative-ion vacancies and n_e is the concentration of electrons in the conduction band. Commercially available alkali halide crystals contain at least 10^{17} cm^{-3} impurity traps, and hence, in analogy to the case of photoconductivity in "dirty" semiconductors, n_e can be expected to vary linearly with the incident power density S . Therefore, one can write

$$c = B_V A S, \quad (4.2)$$

where A is the proportionality constant between n_e and S and, as shown in the Appendix, has a value of the order of 10 in the cgs system of units for KCl at room temperature under the assumption that the concentration of traps is 10^{17} cm^{-3} . On the basis of a classical calculation by Pekar,²⁹ also discussed in the Appendix, one can estimate that $B_V \approx 2.6 \times 10^{-6}$ cm^3/sec . Hence, for the range of intensities used in the coloration experiments (1 to 250 $\text{erg cm}^{-2}/\text{sec}$) c has a value between $0.3 \times 10^{-4}/\text{sec}$ and $65 \times 10^{-4}/\text{sec}$. It is this range of values to which the bleaching rate β must be compared.

Schultz,³⁰ in performing experiments on the coloration of KCl by electrons with energies of the order of 10 MeV, observed a significant self-bleaching of the F centers so generated. The general characteristics of this effect are displayed in Fig. 16. As can be seen, for F -center concentrations greater than approximately 10^{16} cm^{-3} bleaching occurs after each electron pulse.

TABLE II. Data from the measurements of the influence of plastic deformation on the slow-stage coloration rate, $(\Delta n_F/\Delta t)/S$.

% deformation	F -center concentration at which measurement of $\Delta n_F/\Delta t$ was begun. (10^{16}cm^{-3})	$(\Delta n_F/\Delta t)/S$ ($10^{10} \text{cm}^{-3}/\text{erg cm}^{-2}$)	Crystal thickness (cm)
0.8	4.70	2.84	0.075
1.5	4.11	1.91	0.088
1.5	4.84	2.45	0.090
3.1	6.68	3.67	0.080
4.6	7.03	3.75	0.076
6.2	8.55	1.98	0.100
7.7	8.60	4.05	0.117
7.7	8.68	3.71	0.122
9.2	9.95	3.59	0.132
10.8	9.72	2.94	0.126
11.0	10.70	3.26	0.140

²⁸ S. I. Pekar, *Untersuchungen über die Electrontheorie der Kristalle* (Akademie-Verlag, Berlin, 1954), cited in W. E. Bron and W. R. Heller, *Phys. Rev.* **119**, 1864 (1960).

³⁰ H. Schultz, 1961 (private communication); thesis, University of Pennsylvania, 1962 (unpublished).

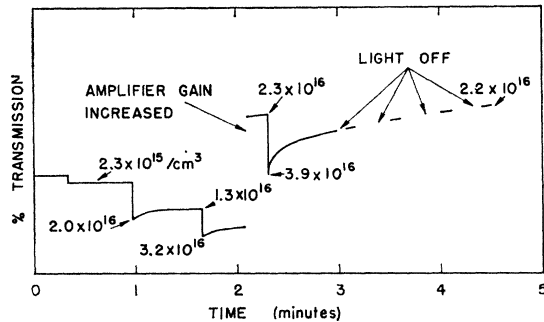


FIG. 16. General characteristics of the self-bleaching of electron-irradiated KCl at room temperature. The ordinate is the optical transmission at the peak of the F band. The vertical lines represent the generation of F centers by $4.5 \mu\text{sec}$ electron pulses during which the energy deposition rate was approximately 80 kW/cm^2 , and the numbers give the calculated F -center concentrations before and after these pulses. The measuring light was turned off during the indicated intervals. (Schultz, reference 30.)

Since this bleaching took place even in total darkness, it cannot be attributed to the effects of light. Schultz found that the self-bleaching at 23°C could be quantitatively described by two bleaching rates, $2100 \times 10^{-4}/\text{sec}$ and $33 \times 10^{-4}/\text{sec}$, with approximately 70% of the bleaching occurring at the latter rate. By comparing the observed efficiency of F -center generation with the efficiency calculated from the cross section for direct ion displacement by relativistic electrons, he came to the conclusion that direct displacement accounted for a negligible portion of the damage. Hence, it is reasonable to assume that the F centers investigated by Schultz are of the same nature as those produced in typical low-energy x-ray coloration experiments, and that the value of β to be used in Eq. (4.1) may be equal to or greater than c .

On the basis of the observed dependence of the strain rate on the intensity of irradiation, one can let $a = gS$. Equation (4.1) can now be rewritten in a form which explicitly displays its intensity dependence, that is, as

$$a^* = B_V A g S^2 / (\beta + B_V A S). \quad (4.3)$$

By taking the derivative of the logarithm of this last equation, one can readily verify that the slope of a log-log plot of a^* vs S is given by

$$\text{slope} = 2 - S / (S + \beta / B_V A). \quad (4.4)$$

At very low intensities such that $S \ll \beta / B_V A$, the slope is approximately equal to two, while at high intensities it is approximately unity. At intermediate intensities a log-log plot of a^* vs S over two decades of S would, when fitted with a straight line, yield a slope between the limits of one and two. As indicated by the values of c and β quoted above, the intensity used in this investigation was of an intermediate value, and hence a value of approximately 1.5 for the slope is reasonable.

An examination of the data presented by Mitchell *et al.* reveals that their intensities were of an intermedi-

ate and somewhat lower value, and hence the above analysis might also serve to explain their observation of an approximately square dependence of F -center generation rate on radiation intensity.

It is interesting to note that significant self-bleaching could also explain the magnitude of $(\Delta n_F / \Delta t) / (\Delta \epsilon / \Delta t)$ indicated in Fig. 13. As is shown in the next section, it is highly unlikely that the ratio between the strain rate and the rate of generation of vacancies in KCl could be greater than approximately $2 \times 10^{-23} \text{ cm}^3$ no matter what the damage mechanism may be. If all of the vacancies generated were converted to F centers, then $(\Delta n_F / \Delta t) / (\Delta \epsilon / \Delta t)$ should not be smaller than $5 \times 10^{22} \text{ cm}^{-3}$. Figure 13 shows that for the lowest intensity used this ratio is, in fact, $1.5 \times 10^{22} \text{ cm}^{-3}$, which clearly implies that all of the vacancies generated do not become stable F centers.

B. Mechanism of Defect Formation

It is of interest to attempt to determine which of the proposed damage mechanisms might be the principal contributor to the external dilation observed in this investigation. In order to do this, the experimental observations may be compared to the behavior predicted by each mechanism.

The lack of dependence of the coloration rate on deformation argues against both the dislocation-jog mechanism¹⁴⁻¹⁶ and the mechanism involving the successive recombination of two excitons at the same site on a dislocation line.² Furthermore, the square law for vacancy generation predicted by this latter mechanism was not observed. The bulk multiple ionization mechanisms,¹⁷⁻²¹ however, are consistent with the lack of deformation dependence. Whether or not these mechanisms can be efficient enough to account for the observed strain rate is now discussed.

The discussion can be separated into three parts: the rate at which chlorine ions become multiply ionized, the probability that a multiply ionized ion will be displaced, and the relationship between the external strain and the concentration of generated vacancies. It will be assumed here that vacancy generation follows multiple ionization with unit probability, and hence the rate of vacancy generation can be taken to be equal to the rate of multiple ionization. Although it is doubtful that this assumption is exactly true, it should be sufficiently accurate for an order-of-magnitude calculation. The multiple ionization itself can come about in two ways: by an inner shell ionization followed by an Auger transition, or by two successive, independent single ionizations. These two processes will now be considered in turn.

Let the rate per unit incident power density at which a given chlorine ion in a KCl lattice suffers inner shell ionization followed by an Auger transition be represented by Q_A . Then the rate of generation of vacancies

per unit volume \dot{n}_v is given by

$$\dot{n}_v = Q_A n_h S, \quad (4.5)$$

where S is the incident power density and n_h is the concentration of chlorine ions. If the strain associated with the generation of a vacancy be represented by the parameter γ , then the specific strain rate predicted by a multiple ionization mechanism initiated by an inner shell ionization followed by an Auger transition $\dot{\epsilon}/S$ can be written as

$$\dot{\epsilon}/S = \gamma Q_A n_h. \quad (4.6)$$

Although γ cannot be calculated precisely, an estimate of its upper limit can be made. The type of defect usually associated with the multiple ionization mechanisms is the Frenkel defect, in which the displaced ion becomes situated in an interstitial position not far removed from the vacancy left behind. Since this configuration automatically preserves local charge neutrality, the generation of negative-, and position-ion vacancies in pairs is not required; hence it is expected that the maximum dilation which can be associated with one induced vacancy is just the volume occupied by a negative ion. For KCl, then, we choose $\gamma(\text{bulk}) \approx 10^{-23} \text{ cm}^3$. Q_A is estimated in the Appendix, the value obtained being $Q_A \approx 5 \times 10^{-12} / \text{erg cm}^{-2}$. Then, using the value $n_h \approx 1.6 \times 10^{22} \text{ cm}^{-3}$, we obtain $\dot{\epsilon}/S \approx 8 \times 10^{-13} / \text{erg cm}^{-2}$. The agreement between this estimated value and the experimentally observed value of $(\Delta\epsilon/\Delta t)/S \approx 7 \times 10^{-13} / \text{erg cm}^{-2}$ is quite favorable, and hence a multiple ionization mechanism initiated by an inner shell ionization followed by an Auger transition can account for the observed dilation. Four different detailed sequences of events by means of which multiple ionization can lead to the displacement of an ion have been proposed.^{17,19-21} It is not possible on the basis of the experiments performed to select one of these sequences as the most probable.

If the multiple ionization takes place through two successive interactions, the situation is somewhat different. Let the rate per unit incident power density at which a given chlorine ion suffers ionization not followed by an Auger transition be represented by Q_S . If such an ionization event takes place, a neutral chlorine will be produced. This neutral chlorine will remain until it either captures an electron (in a characteristic time τ) or suffers another ionization. It is presumed that vacancy generation follows this second ionization with unit probability. Since it does not matter whether the second ionization is followed or not followed by an Auger transition, it is described by $Q_S + Q_A$. By obtaining the steady-state solutions to the differential rate equations corresponding to the above events, it can be shown³¹ that the specific strain rate for this type of process is

given by

$$\frac{\dot{\epsilon}}{S} = \gamma \frac{Q_S(Q_S + Q_A)n_h S}{(2Q_S + Q_A)S + 1/\tau}. \quad (4.7)$$

Although this equation seems to indicate that the specific strain rate is a function of S , let us examine it, and in particular the electron recapture time τ , in further detail.

Clearly τ must refer to the time required for a neutral chlorine to capture an electron from the conduction band since hole migration to a neighboring ion would not alter the concentration of neutral chlorines. Howard and Smoluchowski³² have investigated this time for doubly ionized centers. If one chooses 2.13 for the dielectric constant of KCl and $3 \text{ cm}^2/\text{V sec}$ ³³ for the electron mobility, the application of their method to a singly ionized center yields the expression $\tau \approx 4 \times 10^5/n_e$ sec, where n_e is the concentration of conduction band electrons in the units cm^{-3} . As mentioned in the preceding section, and as demonstrated in the Appendix, $n_e \approx 10 S$ in the cgs system of units. Hence $1/\tau$ is proportional to S , and the intensity dependence drops out of the right-hand side of Eq. (4.7). Finally, then, by using the value $Q_S \approx 12 \times 10^{-11} / \text{erg cm}^{-2}$ (estimated in the Appendix) and previously quoted values of the other parameters, one obtains $\dot{\epsilon}/S \approx 10^{-16} / \text{erg cm}^{-2}$. Since this is three orders of magnitude smaller than the observed strain rate, it is doubtful that a multiple ionization mechanism initiated by two successive interactions contributed significantly to the generation of vacancies in the crystals used in this experiment.

It is also of interest to consider the efficiency of the dislocation-jog mechanism, particularly since there is no *a priori* reason why it cannot occur, and since many investigators have reported a deformation dependence of the coloration rate.^{2,12,34-36} The mathematical description of this process is similar to that leading to Eq. (4.6), the only differences being in the value of γ and the rate at which excitons recombine at a given jog site. Since this mechanism implies the creation of Schottky defects which, for the preservation of local charge neutrality, require that negative- and positive-ion vacancies be produced in pairs, it is reasonable to assume that γ (dislocation) $\approx 2 \times 10^{-23} \text{ cm}^3$. The rate of exciton recombination at a given jog site involves the rate of generation of excitons and the probability that an exciton will live to reach the jog site and there recombine. This latter probability, in turn, depends on both the ratio of impurity and other isolated defects to dislocation jogs and the relative effectiveness of these various defects for causing recombination. Detailed estimates³¹

³¹ E. Abramson, thesis, University of Pennsylvania, 1962 (unpublished).

³² R. E. Howard and R. Smoluchowski, Phys. Rev. **116**, 314 (1959).

³³ H. Kawamura and M. Onuki, J. Phys. Soc. Japan **10**, 162 (1955).

³⁴ A. S. Nowick, Phys. Rev. **111**, 16 (1958).

³⁵ W. E. Bron, Phys. Rev. **119**, 1853 (1960).

³⁶ C. L. Bauer and R. B. Gordon, Phys. Rev. **126**, 73 (1962); Bull. Am. Phys. Soc. **6**, 113 (1961).

show that if one assumes 10^{17} cm $^{-3}$ isolated defects and 10^{13} cm $^{-3}$ jog sites (10^6 dislocation lines/cm 2 with 10^7 jogs/cm on each line), in order that the dislocation-jog mechanism be efficient enough to compete with one of the multiple ionization mechanisms it must also be assumed that jog sites are 100 times more effective in causing exciton recombination than are isolated defects. Possibly, it is the great structure sensitivity of this dislocation-jog mechanism which is responsible for the reported variations in the deformation dependence of the coloration rate in these crystals.

C. Influence of Plastic Deformation

Figure 14 indicates that as a consequence of linear compression of about 8% the crystals actually contract during irradiation. This effect was reproducible and could not be traced to errors arising in the measuring apparatus, and hence it is believed to be real. It has been reported³⁷ that up to about 11% linear compression KCl crystals deform primarily along simple slip systems. Above this relative compression, however, multiple-slip systems become evident. At the same time, above this critical deformation the crystals show a rapid decrease in density (or volume expansion) with increasing deformation. This density change can be completely annealed out by heating the crystal to 350°C. It is possible that the contraction displayed in Fig. 14 is a consequence of the absorbed radiation being effective in activating a relaxation of the volume expansion produced by excessive plastic deformation. If this is indeed true, then there is little hope that strain measurements offer a reliable tool for studying the effect of plastic deformation on the production of vacancies by radiation.

Figure 15 indicates that linear plastic deformation of our KCl crystals has little effect on their slow-stage coloration rate. This is apparently in contradiction to the results of other investigators.^{2,12,34-36} However, in these other investigations, with the exception of those carried out by Mitchell *et al.*, the samples received a relatively low x-ray dose, being irradiated to only just beyond the knee of their growth curves. It is possible that the vacancies generated by moving dislocations during the deformation process can have a marked influence on the total coloration in the region of the knee. Indeed, as evidenced by Table II, our crystals also show a correlation between percent deformation and the value of the *F*-center concentration at which the measurement of the slow-stage coloration rate $\Delta n_F/\Delta t$ was begun. Since all of the samples had approximately the same irradiation history up to this point, the correlation is most probably a reflection of the increased *F*-center concentration at the end of the fast stage of coloration. (Since it is to be expected that *all* of the initially present vacancies will eventually be converted to

F centers, no matter what their position in the crystal, it is not surprising that no thickness effect is evident here.)

The discrepancy between our deformation results and those reported by Mitchell *et al.* cannot be resolved by the foregoing argument since their measurements were also carried out far into the slow stage of coloration. However, as discussed at the end of the preceding section, the impurity concentration of a given sample should have a pronounced effect on the possible contribution of a dislocation mechanism to the total slow-stage coloration rate. Hence, if our crystals were more impure than those used by Mitchell *et al.*, ours would be expected to exhibit less deformation-dependent coloration.

D. Summary

The leading observations and conclusions of this investigation can be summarized as follows:

The observation that the coloration rate of KCl crystals varies as the intensity of irradiation to a power greater than one but less than two, while the rate of generation of vacancies appears to be linear in the intensity, can be explained on the basis of a significant self-bleaching of radiation-induced *F* centers reported by Schultz. Data on the magnitude of the ratio between the slow-stage rate of *F*-center generation and the external strain rate indicates that all of the generated vacancies do not become converted with unit probability to stable *F* centers. This observation is also consistent with self-bleaching.

Our results suggest that the principal contribution to the x-ray damage observed in the particular Harshaw crystals of KCl used in this experiment came from a bulk multiple ionization mechanism initiated by an inner shell ionization followed by an Auger transition. The factors supporting this conclusion are that: (1) This type of mechanism is consistent with the observed lack of dependence of the coloration rate on plastic deformation, and (2) it is the only mechanism so far proposed which is clearly efficient enough to account for the observed radiation-induced external strain.

APPENDIX

A. Estimation of Ionization Rates

In this part of the Appendix, estimates are made of the rate per unit incident power density at which a given chlorine ion in a KCl lattice suffers ionizations both followed and not followed by an Auger transition. The method of attack to be used was suggested by Howard, Vosko, and Smoluchowski.^{2,1}

The electron ejected from an atom during an ionization process may come from any of the electronic shells, provided that sufficient energy is available. If the electron is ejected from an inner shell, one of the electrons in an outer shell will shortly fall into the hole left behind.

³⁷ W. H. Vaughan, W. J. Leivo, and R. Smoluchowski, *Phys. Rev.* **110**, 652 (1958).

Dexter and Beeman³⁸ estimate that a transition of this type to the K shell of argon will occur in about 10^{-15} sec; the situation in chlorine should not be very much different. The downward transition may proceed either radiatively or nonradiatively. In the latter case (the Auger transition) the available energy is carried off by a second electron ejected from the shell from which the downward transition commenced.

The primary ionization of an atom by a photon of energy E results in the ejection of an electron with a kinetic energy $(E - I_\alpha)$, where I_α is the ionization potential of the shell from which the electron was ejected ($\alpha = K, L, M$ for chlorine or for a positive potassium ion). In addition, electrons ejected via the Auger effect have an energy equivalent to $(I_\alpha - 2I_\beta)$, where β refers to the shell from which the downward transition originated. In chlorine, 90% of the photoionizations by 20 keV x rays occur from the K shell,^{39,40} which has an ionization potential of approximately 3 keV. The ejected electrons themselves have sufficient energy to eject a large number of electrons from other atoms by impact ionization. The relative probability of impact ionization from a given shell is given by²⁰

$$p_\alpha = (m_\alpha/I_\alpha) / (\sum m_\alpha/I_\alpha), \quad (\text{A1})$$

where m_α is the number of electrons in the α shell. By using the values: $m_K = 2$, $m_L = m_M = 8$, $I_K = 2830$ eV, $I_L = 217$ eV, and $I_M = 9.6$ eV, one obtains the result that $p_K = 0.0008$, $p_L = 0.042$, and $p_M = 0.957$ for the Cl^- ion. The relative probabilities for the K^+ ion are of the same order of magnitude. As can be seen, most of the secondary ionizations occur from the L and M shells. Since the ionization energies of these shells are considerably smaller than I_K , each secondary electron extracts, on the average, a comparatively small energy from the primary photoelectron. Hence, electron impact accounts for the great majority of the ionization events.

Since p_K is very small compared to the other two probabilities, impact ionizations from the K shell can be neglected. If it is further assumed that in chlorine the Auger ejection of an M electron always follows an L ionization,⁴¹ then the rate at which chlorine ions suffer ionization followed by an Auger transition, R_A , is given by

$$R_A \approx p_L R_i, \quad (\text{A2})$$

and the rate at which chlorine ions suffer ionization not followed by an Auger transition, R_S , is given by

$$R_S \approx p_M R_i, \quad (\text{A3})$$

where R_i is the total rate at which chlorine ions suffer ionization from any shell. If R_e is the rate of generation of conduction band electrons, then, if it is assumed that half of the ionizations in the crystal occur on chlorine ions, R_i can be written as

$$R_i \approx R_e / 2 \langle n \rangle, \quad (\text{A4})$$

where $\langle n \rangle$ is the average number of electrons excited per chlorine ionization and is given by

$$\langle n \rangle \approx 4p_K + 2p_L + p_M. \quad (\text{A5})$$

This last equation assumes that all electron ejections from an inner shell are followed by an Auger transition from the next-highest shell.

Let the rate of energy deposition per unit volume in the crystal be given by $S\mu$, where S is the incident power density and μ is the linear absorption coefficient. Then, under the assumption that the absorbed energy raises the maximum possible number of electrons to the conduction band, R_e can be written as

$$R_e \approx S\mu / (1.5E_g), \quad (\text{A6})$$

where E_g is the band gap or first ionization potential. The factor 1.5 arises from the fact that an electron with a kinetic energy less than E_g cannot cause ionization and itself remain in the conduction band. On the average, then, the lowest kinetic energy to which an initially "hot" electron can descend via impact ionization losses is approximately $\frac{1}{2} E_g$. Hence, each excited electron can be thought of as having extracted an energy equal to approximately $E_g + \frac{1}{2} E_g$ from the absorbed photon.

The rate per unit incident power density at which a specific chlorine ion suffers ionization events is given by $R_i / S n_h$, where n_h is the concentration of chlorine ions. Thus, by using the preceding equations of this section, one can readily verify that

$$Q_A \approx p_L \mu / 3E_g \langle n \rangle n_h \quad (\text{A7})$$

and

$$Q_S \approx p_M \mu / 3E_g \langle n \rangle n_h, \quad (\text{A8})$$

where Q_A and Q_S are the parameters introduced in Section IVB.

The value of μ to be used in the above equations can be chosen from Fig. 5 as follows: The dilatometer used in this investigation measured only the maximum strain in the crystal, which occurred near the front surface. The range of 20 keV electrons in KCl is approximately 4×10^{-4} cm,⁴² and hence a large fraction of the primary photoelectrons generated in a surface layer of this thickness will escape from the crystal. It therefore seems that a reasonable estimate of the value of μ is that corresponding to a depth of approximately 0.001 cm. By performing an extrapolation on Fig. 5, one obtains the order-of-magnitude value $\mu \approx 100$ cm⁻¹. Then, by using the value $n_h \approx 1.6 \times 10^{22}$ cm⁻³ and the other values cited

³⁸ D. L. Dexter and W. W. Beeman, *Phys. Rev.* **81**, 456 (1951).

³⁹ H. A. Bethe and J. Ashkin, in *Experimental Nuclear Physics*, edited by E. Segre (John Wiley & Sons, Inc., New York, 1953), Vol. 1, p. 166ff.

⁴⁰ H. Hall, *Rev. Mod. Phys.* **8**, 358 (1936).

⁴¹ Measurements or calculations in direct support of this assumption could not be found, but see the discussions on this point in references 20 and 31.

⁴² W. John, in *American Institute of Physics Handbook* (McGraw-Hill Book Company, Inc., New York, 1957), pp. 8-38.

above, one obtains $Q_A \approx 5 \times 10^{-12}$ /erg cm^{-2} and $Q_S \approx 12 \times 10^{-11}$ /erg cm^{-2} to an order of magnitude.

A method of estimating the absolute number of impact ionization events from a given inner shell which result from the complete absorption of an electron with a given initial kinetic energy has recently been developed by Durup and Platzman.⁴³ A rough application of their method to our situation yields a value for Q_A of the same order of magnitude as that estimated above.

B. Concentration of Conduction Band Electrons

In this section, an estimate of the relationship between the steady-state concentration of conduction band electrons in typical commercial KCl crystals and the incident x-ray power density will be made. Only a summary of a detailed calculation made elsewhere³¹ will be given.

The differential rate equation obeyed by the conduction band electrons can be written as

$$\dot{n}_e = R_e - n_e(B_i n_e + B_T n_T), \quad (\text{A9})$$

where n_e is the conduction electron concentration, R_e is the rate at which electrons are being raised into the conduction band as given by Eq. (A6), n_T is the concentration of imperfection traps, B_T is the capture coefficient for electrons by these traps, and B_i is the capture coefficient for electrons by the holes residing on ionized ions. The small concentration of multiply ionized ions has been neglected. Although the steady-state solution of the above equation can be obtained in explicit form, the procedure is somewhat simplified if the assumption that $B_i n_e \ll B_T n_T$, which can later be checked for consistency, is made. In this case, the solution becomes

$$n_e \approx 2\mu S / 3E_g B_T n_T. \quad (\text{A10})$$

According to Bron and Heller, Pekar²⁹ has made a classical calculation of the capture coefficients in two

⁴³ J. Durup and R. L. Platzman, *Discussions Faraday Soc.* **31**, 156 (1961).

limiting cases: one in which the capture rate is limited by the transition time into the bound state, and one in which the capture rate is limited by the diffusive motion of the electron. Since in ionic crystals the electron mobility is low and electron-lattice interactions are fairly strong, the latter case is the one most likely to correspond to the process in KCl. Pekar obtains for charged centers

$$B_c = 4\pi e \mu_e / \kappa, \quad (\text{A11})$$

and for neutral centers

$$B_n = 1.1 (4\pi \mu_e) (kT)^{3/4} (\alpha / 2\kappa^2 e^2)^{1/4}, \quad (\text{A12})$$

where μ_e is the electron mobility, κ is the dielectric constant of the crystal, α is the polarizability of the neutral center, and the other parameters have their usual meaning. Using $\mu_e \approx 3 \text{ cm}^2/\text{V sec}$ ³³, $\kappa = 2.13$, $\alpha \approx 5 \times 10^{-23} \text{ cm}^3$, and $T = 300^\circ\text{K}$, one obtains $B_c \approx 2.6 \times 10^{-6} \text{ cm}^3/\text{sec}$ and $B_n \approx 4.4 \times 10^{-8} \text{ cm}^3/\text{sec}$. These values are in relatively good agreement with those estimated from photoconductivity data.⁴⁴

The imperfection traps represented by n_T initially consist of vacancies present before irradiation and impurities, and together have a typical concentration of 10^{17} cm^{-3} . It has been shown in the detailed calculations³¹ that as the total radiation dose received by the crystal increases, these traps become filled and are replaced by traps associated with ionized ions, the total number of traps remaining essentially constant. Hence, the best selection of a value for B_T is most probably that given by B_c above. Insertion of these values and the values of the other parameters as cited in the preceding section into Eq. (A10) yields the result that, to an order of magnitude, $n_e \approx 10S$ in the cgs system of units for KCl at room temperature. It can readily be verified that for the incident power densities used in this experiment ($S \approx 100 \text{ erg cm}^{-2}/\text{sec}$) the solution is consistent with the assumption that $B_i n_e \ll B_T n_T$.

⁴⁴ H. U. Harten, *Z. Physik* **126**, 619 (1949); G. Glaser and W. Lehfeldt, *Nachr. Akad. Wiss. Göttingen, Math.-Physik Kl.* **2**, 91 (1936); see discussion in Appendix C of reference 31.